

Electronic Supplementary Information

From coconut shell to porous graphene-like nanosheets for high-power supercapacitor

*Li Sun, Chungui Tian, Meitong Li, Xiangying Meng, Lei Wang, Ruihong Wang, Jie Yin and Honggang Fu **

Key Laboratory of Functional Inorganic Material Chemistry, Ministry of Education of the People's Republic of China, Heilongjiang University, Harbin 150080 P. R. China

Corresponding author E-mail: fuhg@vip.sina.com,

Tel.: +86 451 8660 4330, Fax: +86 451 8667 3647

Table S1. The detailed experimental parameters for different samples.

Sample	Mass ratio of ZnCl ₂ /coconut shell	Carbonization temperature	Concentration of FeCl ₃ (M)
PGNS-3-700	3	700	3
PGNS-3-800	3	800	3
PGNS-3-900	3	900	3
PGNS-3-1000	3	1000	3
PGNS-1-900	1	900	3
PGNS-5-900	5	900	3
GC-900	0	900	3
AC-900	3	900	0

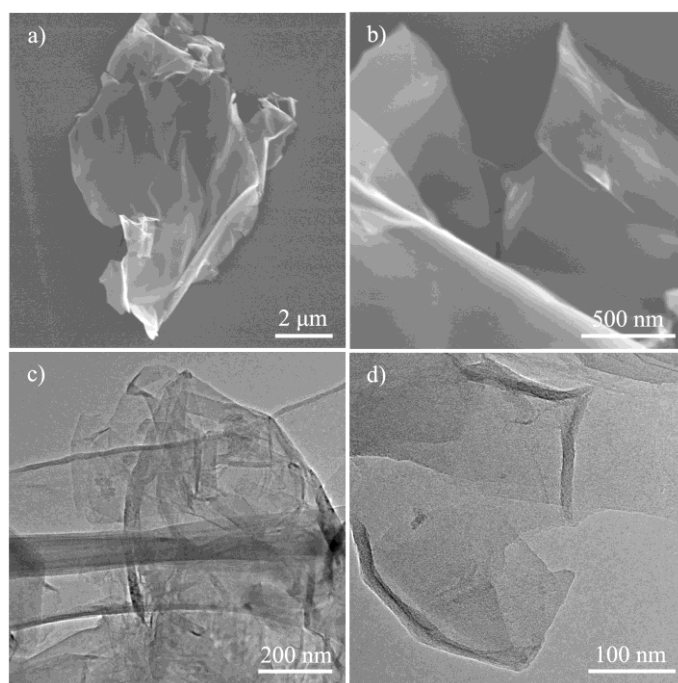


Fig. S1 a, b) SEM and c, d) low-magnification TEM images of the porous graphene-like nanosheets (PGNS-3-900).

Table S2 The values of I_G/I_D calculated based on the Raman results for the different samples.

Sample	I_G/I_D
PGNS-3-700	1.76
PGNS-3-800	1.81
PGNS-3-900	3.98
PGNS-3-100	5.23
0	
PGNS-1-900	4.01
PGNS-5-900	3.87
GC-900	5.69
AC-900	0.97

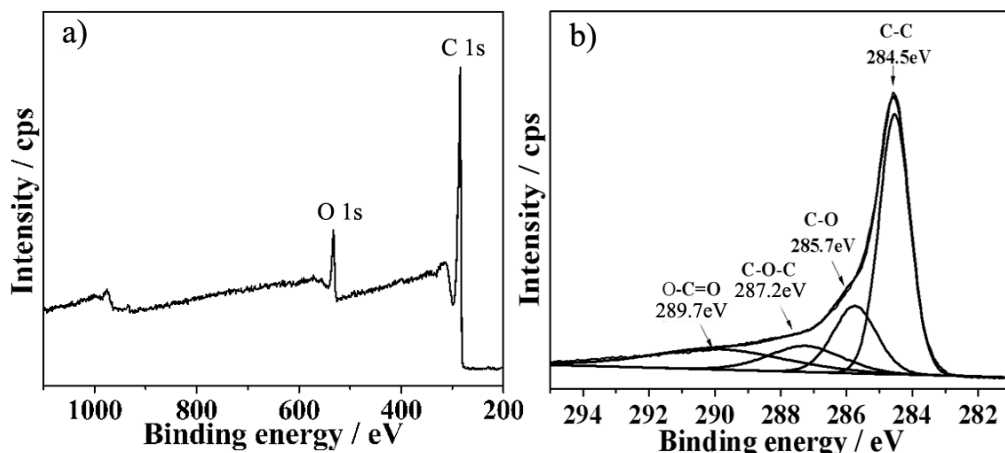


Fig. S2 XPS spectra of PGNS-3-900: a) survey spectrum and b) high-resolution C 1s spectrum.

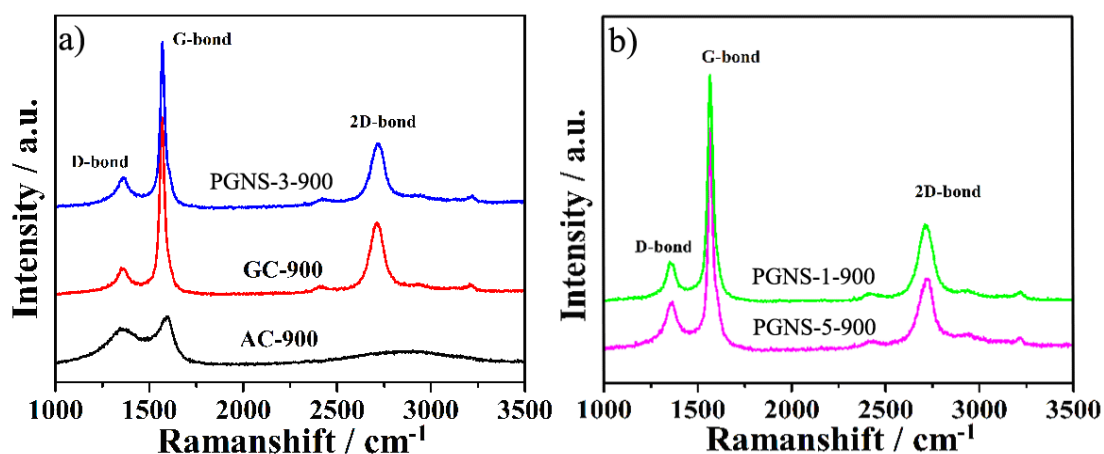


Fig. S3. a) Raman spectra of PGNS-3-900, GC-900 and AC-900; b) Raman spectra of PGNS-1-900 and PGNS-5-900 sample.

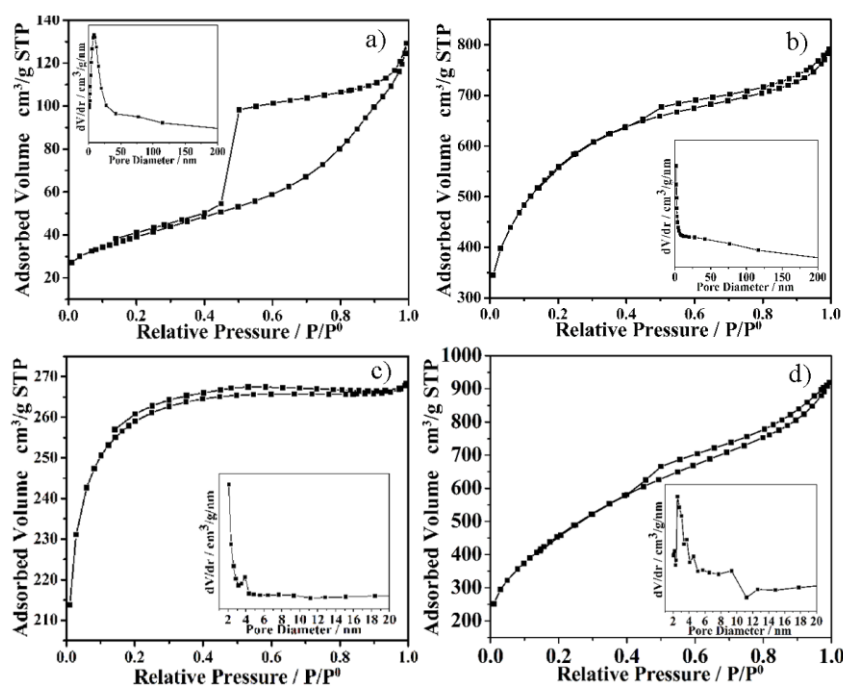


Fig. S4. Nitrogen adsorption/desorption isotherms and pore size distribution (inset) of a) GC-900, b) AC-900, c) PGNS-1-900 and d)PGNS-5-900 materials.

Table S3 Structural parameters extracted from the curve fitting of XRD spectra

Samples	$2\theta_{002}$ (deg.)	$2\theta_{100}$ (deg.)	d_{002} (nm)	L_c (nm)	L_a (nm)
PGNS-3-800	26.45	44.57	0.3378	19.9274	22.0105
PGNS-3-900	26.53	44.61	0.3353	23.9310	24.8033
PGNS-3-1000	26.59	44.63	0.3346	24.6889	28.3129

The Lateral size (L_a) and the stacking height (L_c) of the crystallite are determined using the equation:

$$d_{002} = \lambda / (2 \sin \theta_{002}) \quad (1)$$

$$L_c = 0.89 \lambda / (B_{002} \cos \theta_{002}) \quad (2)$$

$$L_a = 1.84 \lambda / (B_{100} \cos \theta_{100}) \quad (3)$$

Where λ is the wavelength of X-ray used (Cu K_a, $\lambda=0.15406\text{nm}$), B_{100} and B_{002} are the half width of the (100) and (002) peaks and θ_{100} and θ_{002} are the corresponding scattering angles.

Table S4. S_{BET} and specific capacitances of the studied samples under different experimental conditions calculated from charge/discharge curves measured at different current densities.

Samples	S_{BET} ($\text{m}^2 \text{ g}^{-1}$)	C_g (F g^{-1})				
		1 A g^{-1}	5 A g^{-1}	10 A g^{-1}	20 A g^{-1}	30 A g^{-1}
PGNS-3-700	1281	168	137	129	119	100
PGNS-3-800	1519	214	185	161	143	129
PGNS-3-900	1874	268	227	214	200	185
PGNS-3-1000	1538	237	197	175	153	137
GC-900	138	117	101	95	82	79
AC-900	2007	210	176	166	147	108

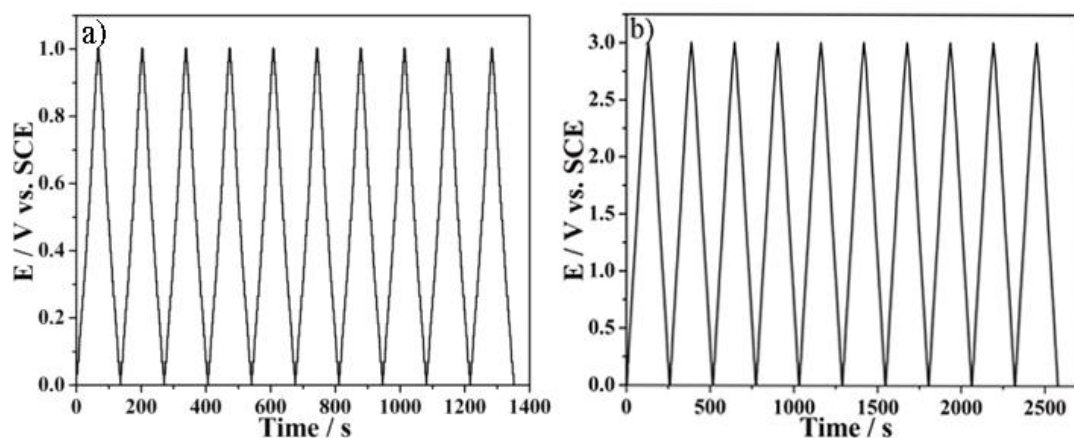


Fig. S5. a) and b) are the galvanostatic charge/discharge curves of PGS-3-900 tested at 1 A g^{-1} in 6 M KOH and 1 M $\text{Et}_4\text{NBF}_4\text{-PC}$ electrolytes, respectively.